Received January 29, 2019, accepted March 7, 2019, date of publication March 14, 2019, date of current version April 2, 2019.

Digital Object Identifier 10.1109/ACCESS.2019.2904966

Analysis of Underlaid D2D-Enhanced Cellular Networks: Interference Management and Proportional Fair Scheduler

JUNNAN YANG[1], (Student Member, IEEE), MING DING[2], (Senior Member, IEEE), GUOQIANG MAO[3], (Fellow, IEEE), ZIHUAI LIN[4], (Senior Member, IEEE), AND XIAOHU GE[5], (Senior Member, IEEE)

[1]School of Electrical and Data Engineering, University of Technology Sydney, Sydney, NSW 2007, Australia
[2]Data61, CSIRO, Sydney, NSW 2015, Australia
[3]School of Computing and Communications, University of Technology Sydney, Broadway, NSW 2007, Australia
[4]School of Electrical and Information Engineering, The University of Sydney, Sydney, NSW 2006, Australia
[5]School of Electronic Information and Communications, Huazhong University of Science and Technology, Wuhan 430074, China

Corresponding author: Guoqiang Mao (g.mao@ieee.org)

ABSTRACT Device-to-device (D2D) communications have been proposed as a promising technology to improve network capacity and user experiences in the future mobile networks such as heterogeneous networks with densely deployed small cells, but it has not yet been fully incorporated into the existing cellular networks. Interference management is one of the critical issues when D2D communications using uplink resources and coexisting with conventional cellular communications, especially in the ultra-dense networks (UNDs). In this paper, we address the critical issue of interference management by a mode selection method, which is based on the maximum received signal strength (MRSS) for each D2D transmitter (TU). To analyze the capacity of a more practical D2D-enhanced network, we consider that the typical user is no longer a random user, i.e., random user selection by a round-robin (RR) scheduler, as assumed in most studies in the literature. Instead, a cellular user with the maximum proportional fair (PF) metric is chosen by its serving base station as the typical user, which is referred to as the PF scheduler in the cellular tier. Furthermore, we theoretically study the performance in terms of the coverage probability and the area spectral efficiency (ASE) for both the cellular network and the D2D one with the consideration of the PF scheduler in UDNs. Analytical results are obtained, and the accuracy of the proposed analytical framework is validated through Monte Carlo simulations. Through our theoretical and numerical analyses, we quantify the performance gains brought by D2D communications and the PF scheduler in cellular networks, and we find an optimum mode selection threshold β to maximize the total ASE in the network.

INDEX TERMS Device-to-device, inter-cell interference (ICI), interference management, line-of-sight (LoS), non-line-of-sight (NLoS), coverage probability, area spectral efficiency (ASE), proportional fair scheduler.

I. INTRODUCTION

In the last decade, there has been an explosive increase in the demand for data traffic [1]. To address such massive consumer demand for data communications, several noteworthy technologies have been proposed [2], such as small cell networks (SCNs), cognitive radio, device-to-device (D2D) communications, etc. As one of the promising technologies, D2D communications allow direct data transfer between a pair of nearby mobile UEs. Due to the short communication distance between such pairs of D2D user equipment (UEs), D2D communications hold great promise in improving network performance such as the coverage, spectral efficiency, energy efficiency and so on [3].

In the standardization of the 5-th generation (5G) networks, the orthogonal frequency division multiple access (OFDMA) based D2D communications adopt two types of spectrum sharing methods, (i) in-band (e.g., using cellular spectrum) or (ii) out-band (e.g., unlicensed spectrum). In particular, in the in-band D2D communications, D2D users can set up

The associate editor coordinating the review of this manuscript and approving it for publication was Adnan Shahid.

their communications in an underlay or overlay manner. More specifically, in an underlying setting, D2D users use the same spectrum of cellular users (CUs) whereas in the overlay, D2D users access a dedicated portion of cellular spectrum [4]. Recently, it has been standardized by the 3rd Generation Partnership Project (3GPP) [5] that Proximity Services (ProSe) should use uplink resources when coexisting with conventional cellular communications. This means that practical D2D communications will underlay with cellular networks in the uplink.

Although the reuse of the cellular spectrum via D2D can improve the area spectral efficiency of the network, such D2D operations also pose great challenges. The major challenge in the D2D-enabled cellular network is the existence of inter-tier and intra-tier interference due to the aggressive frequency reuse, where cellular UEs and D2D UEs share the same spectrum. It is essential to design an effective interference management scheme to control the interference generated by the D2D links to the cellular links, and vice versa. Consequently, there has been a surge of academic studies in this area. Transmission power control [6]–[9], distance-based mode selection [10]–[12] and guard-zone interference control schemes [13]–[15] have been proposed to solve this problem.

On the other hand, as pointed out in [16], one major weakness of recent research on D2D communications is a lack of realistic scenarios for future mobile networks such as heterogeneous networks with densely deployed small cells. As a straightforward way to increase network capacity, the SCN densification also opens up new research questions, especially in the context of D2D communications. First, scheduling has been conceived as an effective use selection technique used at base stations (BSs) to efficiently use the available spectrum and improve the overall system throughput. Second, the path loss models of D2D links and cellular links in a D2D-enabled cellular network are different due to the difference in the heights and the locations of transmitters [17]. Third, It is well known that LoS transmission may occur when the distance between a transmitter and a receiver is small, and non-line-of-sight (NLoS) transmission is common in office environments and in central business districts. When the distance between a transmitter and a receiver decreases, the probability that a LoS path exists between them increases, thereby causing a transition from NLoS transmission to LoS transmission with a higher probability. Due to the proximity between D2D users, the physical channels which constitute D2D communications are expected to be complex, experiencing both LoS and NLoS conditions across these pairs, which are distinctly different from conventional cellular environments [18].

In this paper, we will consider the above network models and will also present a novel mode selection scheme based on the maximum received signal strength for D2D transmitter (TU) to control the interference and focus on the analysis of the orthogonal deployment of uplink sharing D2D-enhanced UDNs. The maximum received signal strength based mode selection scheme is more practical than the distance-based mode selection in most existing studies because in practice it is possible that the strongest received signal strength is not associated with the closest BS but the one with the minimum path loss with a line-of-sight (LoS) link. In more detail, a UE will operate in a cellular mode if its received signal strength from the strongest base station (BS) is larger than a threshold β; otherwise, it will operate in a D2D mode. This will mitigate the overlarge interference from the D2D links to the cellular links. To analyze the proposed framework, we develop a theoretical framework that takes practical path loss model and Rayleigh fading into account. Based on our analytical results, we find a tradeoff between the maximization of the area spectral efficiency (ASE) performance and the fairness of the D2D links, and the optimum setting of the threshold β that maximizes the ASE.

To the best of our knowledge, there has been no prior work on the theoretical study of the D2D-Enhanced dense cellular networks with interference management and the PF scheduler [2]. Our analysis shows a non-trivial difference on the network performance when considering different path loss models for the cellular links and the D2D links respectively, which captures the different environmental conditions that cellular links and D2D links operate in.

Compared with the existing work, the main contributions of this paper are:

- We propose a tractable interference management scheme for each user equipment (UE) to control the co-channel interference. Specifically, a UE will operate in a cellular mode if its received signal strength from the strongest base station (BS) is larger than a threshold; otherwise, it will operate in a D2D mode. Such an interference management scheme mitigates large interference from D2D transmitter to the cellular network. Through our theoretical and numerical analyses, we quantify the performance gains brought by D2D communications in cellular networks and we find an optimum mode selection threshold β to maximize the total ASE in the network.
- We investigate a general D2D-enhanced dense network performance with the consideration of PF schedulers. For the first time, we use stochastic geometry [19] to derive the analytical results of the coverage probability and the area spectral efficiency (ASE) performance of the D2D-enhanced UDNs with PF schedulers used at BSs. The key point of our analysis is that the typical user is no longer a random user as assumed in most exiting studies of stochastic geometry.
- Different from the existing work that does not differentiate the path loss models between cellular links and D2D links, our analysis adopts two different path loss models for cellular links and D2D links, respectively. Our results demonstrate that the D2D links can provide a considerable ASE gain when the threshold parameter β is appropriately chosen. More specifically, our analysis shows the interference from D2D tier can be controlled

by using our mode selection scheme, and there is an optimal to achieve the maximum ASE while the performance of cellular tier is guaranteed.

The rest of this paper is structured as follows. Section II provides a brief review of related work. Section III describes the system model. Section IV presents our theoretical analysis on the coverage probability and the ASE. The numerical and simulations results are discussed in Section V. Our conclusions are drawn in Section VI.

II. RELATED WORK

Device-to-device (D2D) communications underlying cellular networks are ongoing standardization topics in Long Term Evolution Advanced (LTE-A) [5], i.e., in-band D2D, mainly as a means to improve the coverage [3] so that improve the throughput or the spectrum efficiency through traffic offloading from cellular network. There is rich literature in modeling and investigating D2D enabled cellular network. Meanwhile, the stochastic geometry which is accurate in modeling irregular deployment of base stations and mobile user equipment has been widely used to analyze network performance [20]–[26]. Andrews, et al. conducted network performance analyses for the downlink (DL) [20] and the uplink (UL) [21] of SCNs, in which UEs and/or BSs were assumed to be randomly deployed according to a homogeneous Poisson point process (HPPP). In [24], Badri *et al.* proposed joint mode selection and pairing in mixed cellular and D2D network which based on the biased received power from the nearest BS. In [25], modeling and performance analysis of D2D enabled networks with mobility have been presented and a distance-based mode selection scheme has been proposed. In [26], Salehi *et al.* developed an analytical framework for the D2D communications underlying cellular network in the DL in terms of the meta-distribution of the signal-to-interference ratio.

As one of the fundamental problem in the D2D communication system, the management of the interference has been analyzed in the literature [6], [7], [9], [10], [12]–[15]. In [9], Lee *et al.* proposed a power control algorithm to control the co-channel interference in which global channel state information is required at BSs. In [10], Liu *et al.* provided a unified framework to control the interference in a multi-channel environment with Rayleigh fading, where D2D UEs were selected based on the average received signal strength from the nearest BS, which is equivalent to a distance-based selection. A distributed power control scheme has been proposed in [12] to mitigate interference in a D2D underlaid cellular system. In [13], Min *et al.* proposed an interference-limited area control scheme to mitigate the interference from cellular to D2D considering a single slope path loss model. George *et al.* [14] and Lv *et al.* [15] proposed novel approaches to model the interference in uplink or downlink underlaid/overlaid with Rayleigh fading and single path loss model.

Although the existing works have provided precious insights into interference management for D2D communications, there are remaining problems: the mode selection schemes in the literature were not very practical. Note that in some existing works [10], [11], it was assumed that each UE should connect to the nearest BS and select operation mode based on the distance. However, maximum received signal strength based mode selection scheme is more practical than the distance-based mode selection since in practice it is possible that the strongest received signal strength is not associated with the closest BS but the one with the minimum path loss with a LoS link.

On the other hand, as the de facto standard in cellular networks, proportional fair (PF) scheduling has been extensively studied [27]–[29]. In [27], Margolies *et al.* developed the predictive finite-horizon PF scheduling ((PF)2S) framework that exploits mobility. In [29], Hojeij *et al.* proposed a low-complexity waterfilling-based power allocation (PA) technique, incorporated within the proportional fairness scheduler. Nevertheless, there has been no prior work on the theoretical study of the PF scheduler in the context of D2D-enhanced cellular network or UDNs. Generally speaking, the existing work on PF schedulers does not scale well with the network densification. In [30], Choi and Bahk analyzed the PF scheduler to obtain cell throughput in a scenario with merely one BS. In [31], Wu *et al.* studied the PF scheduler in a scenario with a limited number of BSs, which quickly becomes computationally infeasible for UDNs. In [32], only system-level simulations are studied for large-scale networks, which lacks analytical rigor.

To sum up, in this paper, we propose a D2D-enhanced dense cellular network framework which takes into account an interference management scheme based on the maximum received signal strength, probabilistic NLoS and LoS transmissions and the proportional fair scheduler. This work shed new insight on the interference management of coexistent D2D and cellular transmissions and the insight is expected to provide a design guideline for D2D mode selections.

III. SYSTEM MODEL

In this section, we first explain the scenario of the D2D communication coexisting with the cellular network. Then, we present the path loss model, interference management scheme, the PF scheduler and the performance metrics.

A. SCENARIO DESCRIPTION

We consider a D2D underlaid UL cellular network, where BSs and UEs, including cellular uplink UEs and D2D UEs, are assumed to be distributed on an infinite two-dimensional (2D) plane $\mathbb{R}^2$. We assume that the cellular BSs are spatially distributed according to a 2D homogeneous PPP of intensity λ_b, i.e., $\Phi_b = \{X_i\}$, where X_i denotes the spatial locations of the ith BS. For the cellular network, we assume the uplink UEs which only operate in cellular mode are deployed following an arbitrary stationery and ergodic Poisson point process of intensity λ_u. Moreover, the D2D transmitters are also distributed in the network region according to another independent homogeneous PPP Φ_{TU} of intensity λ_{TU}. We assume that each D2D transmitter has a dedicated receiver located at

distance l in a random direction as [26]. In this paper, we take a PF scheduler into account in the cellular tier, which will be described in detail in Subsection III-C.

Furthermore, we assume that each UE and each BS transmit with constant powers P_D and P_B, respectively. Finally, we adopt a unified channel model that only Rayleigh fading h is considered for both cellular and D2D links: where h is the fading factor following an exponential distribution with unit mean, i.e., $h \sim \exp(1)$.

B. PATH LOSS MODEL

In this paper, we incorporate both NLoS and LoS transmissions into the path loss model. Following [17] and [33], path loss functions adopted in the 3GPP [4] for cellular links and D2D links are considered, which can be written as

$$\zeta_B(r) = \begin{cases} A_{BL} r^{-\alpha_{BL}}, & \text{LoS Probability: } \Pr_B^{\mathrm{L}}(r) \\ A_{BN} r^{-\alpha_{BN}}, & \text{NLoS Probability: } 1 - \Pr_B^{\mathrm{L}}(r) \end{cases} \tag{1}$$

and

$$\zeta_D(r) = \begin{cases} A_{DL} r^{-\alpha_{DL}}, & \text{LoS Probability: } \Pr_D^{\mathrm{L}}(r) \\ A_{DN} r^{-\alpha_{DN}}, & \text{NLoS Probability: } 1 - \Pr_D^{\mathrm{L}}(r). \end{cases} \tag{2}$$

Specifically,

$$\Pr_B^{\mathrm{L}}(r) = \begin{cases} 1 - 5\exp(-R_1/r) & 0 < r \le d_B \\ 5\exp(-r/R_2) & r > d_B \end{cases} \tag{3}$$

and

$$\Pr_D^{\mathrm{L}}(r) = \begin{cases} 1 & 0 < r \le d_D \\ 0 & r > d_D \end{cases} \tag{4}$$

where $A_{BL} = 10^{\frac{1}{10}A_{BL}^{\mathrm{dB}}}$ and $A_{BN} = 10^{\frac{1}{10}A_{BN}^{\mathrm{dB}}}$, $A_{DL} = 10^{\frac{1}{10}A_{DL}^{\mathrm{dB}}}$ and $A_{DN} = 10^{\frac{1}{10}A_{DN}^{\mathrm{dB}}}$ are determined by the transmission frequency for BS-to-UE links and UE-to-UE links in LoS and NLoS conditions, respectively. Parameters α_{BL} and α_{BN}, α_{DL} and α_{DN} denote the path loss exponents for BS-to-UE links and UE-to-UE links with LoS and NLoS conditions, respectively. Parameters $R_1 = 156$ m, $R_2 = 30$ m, and $d_B = \frac{R_1}{\ln 10} = 67.75$ m [4]. Parameter $d_D = 50$ m is the cut-off distance of the LoS link for UE-to-UE links.

C. INTERFERENCE MANAGEMENT SCHEME

There are two modes for TUs in the considered D2D-enabled UL cellular network, i.e., cellular mode and D2D mode. Each TU is assigned with an operation mode according to the comparison of the maximum received DL power from its strongest BS with a threshold. In more detail, the considered mode selection criterion is formulated as

$$Mode = \begin{cases} \text{Cellular}, & \text{if } P^* = \max\limits_{\Phi_b} \left\{ P^{\mathrm{rx}}_{\Phi_b} \right\} > \beta \\ \text{D2D}, & \text{otherwise}, \end{cases} \tag{5}$$

where the string variable *Mode* takes the value of 'Cellular' or 'D2D' to denote the cellular mode and the D2D mode, respectively. P^{rx} is the received signal strength from a BS. In particular, for a tagged TU, if P^* is larger than a specific threshold $\beta > 0$. This TU is not appropriate to work in the D2D mode due to its potentially large interference to cellular UEs. Hence, it should operate in the cellular mode and directly connect with the strongest BS, i.e., the BS that offers the highest received signal strength; otherwise, it should operate in the D2D mode. The UEs which are associated with cellular BSs are referred to as cellular UEs (CUs). The distance from a CU to its associated BS is denoted by R_B. From [7], we assume CUs are distributed following a PPP Φ_c.

The received power for a typical TU from a BS b can be written as

$$P_b^{\mathrm{rx}} = \begin{cases} P_B A_{BL} R_B^{-\alpha_{BL}} & \text{LoS} \\ P_B A_{BN} R_B^{-\alpha_{BN}} & \text{otherwise}, \end{cases} \tag{6}$$

where P_B is the transmission power of a BS. Based on the above system model, we can obtain the intensity of CU as $\lambda_c = \lambda_u + p\lambda_{TU}$, where p denotes the probability of $P^* > \beta$ and will be derived in closed-form expressions in Section IV. It is apparent that the TUs operating in D2D mode are distributed following another PPP Φ_d, the intensity of which is $\lambda_d = (1-p)\lambda_{TU}$. We assume an underlay D2D in the UL dense cellular network model. That is, each D2D transmitter reuses the same frequency with cellular UEs, which incurs inter-tier interference from the D2D tier to the cellular tier. However, there is no intra-cell interference between cellular UEs since we assume an orthogonal multiple access technique in a BS.

D. BS ACTIVATION AND UE DISTRIBUTION

In practice, a BS will enter an idle mode if there is no UE connected to it, which reduces the interference to neighboring UEs as well as the energy consumption of the network. The set of active BSs should be determined by a user association strategy (UAS). In this paper, we assume a practical UAS as in [17], where each UE is connected to the BS having the maximum average received signal strength. Note that such BS idle mode operation is not trivial, which even changes the capacity scaling law [34]. Since UEs are randomly and uniformly distributed in the network, we assume that the active BSs also follow an HPPP distribution $\tilde{\Phi}$ [35], the density of which is denoted by $\tilde{\lambda}$ BSs/km^2. Note that $\tilde{\lambda} \le \lambda_b$ and $\tilde{\lambda} \le \lambda_c$, since one UE is served by at most one BS.

From [35] and [36], $\tilde{\lambda}$ is given by

$$\tilde{\lambda} = \lambda_b \left[1 - \frac{1}{\left(1 + \frac{\lambda_c}{q\lambda_b}\right)^q} \right], \tag{7}$$

where according to [36], q depends on the path loss model, but a good approximation is suggested as q = 3.5 [35].

According to [35], the per-BS coverage area size X can be approximately characterized by a Gamma distribution and the probability density function (PDF) of X can be expressed as

$$f_X(x) = (q\lambda_b)^q x^{q-1} \frac{\exp(-q\lambda_b x)}{\Gamma(q)}, \tag{8}$$

where $\Gamma(\cdot)$ is the Gamma function [37]. The UE number per BS is denoted by a random variable (RV) K, and the probability mass function (PMF) of K can be calculated as

$$\begin{aligned} f_K(k) &= \Pr[K=k] \\ &\overset{(a)}{=} \int_0^{+\infty} \frac{(\lambda_c x)^k}{k!} \exp(-\lambda_c x) f_X(x) dx \\ &\overset{(b)}{=} \frac{\Gamma(k+q)}{\Gamma(k+1)\Gamma(q)} \left(\frac{\lambda_c}{\lambda_c+q\lambda_b}\right)^k \left(\frac{q\lambda_b}{\lambda_c+q\lambda_b}\right)^q, \end{aligned} \quad (9)$$

where (a) is due to the HPPP distribution of UEs and (b) is obtained from (8). Note that $f_K(k)$ satisfies the normalization condition: $\sum_{k=0}^{+\infty} f_K(k) = 1$. It can be seen from (9) that K follows a Negative Binomial distribution [37], i.e., $K \sim \mathrm{NB}\left(q, \frac{\lambda_c}{\lambda_c+q\lambda}\right)$.

We assume that a BS with $K = 0$ is not active. Thus, we focus on the active BSs and denote *the UE number per active BS* by a positive RV $\tilde{K}$. Considering (9), we can conclude that $\tilde{K}$ follows a truncated Negative Binomial distribution, the PMF of which is denoted by $f_{\tilde{K}}\left(\tilde{k}\right), \tilde{k} \in \{1, 2, \ldots, +\infty\}$ and can be written as

$$f_{\tilde{K}}\left(\tilde{k}\right) = \Pr\left[\tilde{K}=\tilde{k}\right] = \frac{f_K\left(\tilde{k}\right)}{1-f_K(0)}. \quad (10)$$

Furthermore, the cumulative mass function (CMF) of $\tilde{K}$ can be written as

$$F_{\tilde{K}}\left(\tilde{k}\right) = \sum_{t=1}^{\tilde{k}} f_{\tilde{K}}(t). \quad (11)$$

E. THE PROPORTIONAL FAIR SCHEDULER

The original operation of the PF scheduler is as follows [30],

- First, the average throughput of each CU is tracked by an exponential moving average at the BS.
- Second, each CU frequently feeds back its channel state information (CSI) to its serving BS, so that such BS can calculate the ratio of the instantaneous achievable rate to the average throughput for each user, which is defined as a PF metric for CU selection.
- Finally, the CU with the maximum PF metric will be selected for UL transmission, which is formulated as

$$u^* = \underset{u\in\left\{1,2,\ldots,\tilde{k}\right\}}{\arg\max} \left\{\frac{\tilde{R}_u}{\bar{R}_u}\right\}, \quad (12)$$

where u, u^*, $\tilde{R}_u$ and $\bar{R}_u$ denote the CU index, the selected CU index, the instantaneous achievable rate of CU u and the average throughput of CU u, respectively. Note that the distribution of $\tilde{k}$ has been discussed in (10).

From a network performance analysis point of view, it is very difficult, if not impossible, to analyze the original PF scheduler given by (12). This is because the objective of a performance analysis is usually to derive the average user throughput $\bar{R}_u$ or aggregate inter-cell interference, but in this case it is part of the PF metric, i.e., $\frac{\tilde{R}_u}{\bar{R}_u}$, and it should be known and plugged into the CU selection criterion of (12) before the performance analysis of $\bar{R}_u$ is carried out. A widely adopted approach to tackle this dilemma is to use alternative measures of CSI in a PF metric, instead of $\tilde{R}_u$ and $\bar{R}_u$ [30], [31], [38], [39].

Here, we follow the framework developed in [30], where the authors proposed to use the ratio of the instantaneous signal-to-noise ratio (SNR) to the average SNR as a PF metric instead of the original one. More specifically, the CU selection criterion of the PF scheduler proposed in [30] is given by

$$u^* = \underset{u\in\left\{1,2,\ldots,\tilde{k}\right\}}{\arg\max} \left\{\frac{\tilde{Z}_u}{\bar{Z}_u}\right\}, \quad (13)$$

where $\tilde{Z}_u$ and $\bar{Z}_u$ denote the instantaneous SNR of CU u and the average SNR of CU u, respectively. **Although this criterion of (13) is not exactly the same as that of (12), it captures the essence of the PF scheduler**:

- Allowing preference to CUs with relatively good instantaneous channels with respect to their average ones since $\tilde{R}_u$ *is a strictly monotonically increasing function of* $\tilde{Z}_u$.
- Allocating the same portion of resource to each CU in the long term to enforce fairness, because the chance of $\tilde{Z}_u \geq \bar{Z}_u$ is almost the same for all CUs. Since the accuracy and the practicality of (13) have been well established in [30], we will focus on studying the PF scheduler characterized by (13).

F. PERFORMANCE METRICS

According to [20], we define the coverage probability as a probability that a receiver's signal-to-interference-plus-noise ratio (SINR) is above a pre-designated threshold γ:

$$P_{Mode}(\gamma, \lambda_b, \lambda_u, \lambda_{TU}) = \Pr[\mathrm{SINR} > \gamma], \quad (14)$$

where γ is the SINR threshold, the subscript string variable *Mode* takes the value of 'Cellular' or 'D2D'. The interference in this paper consists of the interference from both cellular UEs and D2D transmitters.

Furthermore, the area spectral efficiency in bps/Hz/km^2 can be formulated as

$$\begin{aligned} &A^{\mathrm{ASE}}_{Mode}(\lambda_{Mode}, \gamma_0) \\ &\quad = \lambda_{Mode} \int_{\gamma_0}^{\infty} \log_2(1+x) f_X(\lambda_{Mode}, \gamma_0) dx, \end{aligned} \quad (15)$$

where γ_0 is the minimum working SINR for the considered network, and $f_X(\lambda_{Mode}, \gamma_0)$ is the PDF of the SINR observed at the typical receiver for a particular value of λ_{Mode}.

For the whole network consisting of both cellular UEs and D2D UEs, the sum ASE can be written as

$$A^{\mathrm{ASE}} = A^{\mathrm{ASE}}_{\mathrm{Cellular}} + A^{\mathrm{ASE}}_{\mathrm{D2D}}. \quad (16)$$

IV. MAIN RESULTS

In this section, the performance of UEs is characterized in terms of their coverage probability and ASE both for the

cellular tier and the D2D tier. The probability that a TU operating in the cellular mode is derived in Section IV-A, the coverage probabilities of cellular UE and D2D UE are derived in Section IV-B1 and Section IV-B2, respectively.

A. THE PROBABILITY OF UE OPERATING IN THE CELLULAR MODE

In this subsection, we present our results on the percentage that the TUs to operate in the cellular mode. In the following, we present our result in Lemma 1, which will be used in the later analysis of the coverage probability.

Lemma 1: The percentage of a TU to operate in the cellular mode p is given by

$$p = 1 - \exp\left[-2\pi\lambda_b\left(\int_0^{\left(\frac{P_B A_{BL}}{\beta}\right)^{1/\alpha_{BL}}} p^L(r) r dr + \int_0^{\left(\frac{P_B A_{BN}}{\beta}\right)^{1/\alpha_{BN}}} p^{NL}(r) r dr\right)\right], \quad (17)$$

the percentage that a TU to operate in the D2D mode is $(1-p)$.

Proof: See Appendix A. ∎

Note that Eq.(17) explicitly account for the effects of Rayleigh fading, path loss, transmit power, spatial distribution of BSs and mode selection threshold β. From the result, we can see that the HPPP ϕ_{TU} can be divided into two PPPs: the PPP with intensity $p\lambda_{TU}$ and the PPP with intensity $(1-p)\lambda_{TU}$, which representing cellular mode TUs and D2D mode TUs, respectively. Same as in [7], We assume these two PPs are independent.

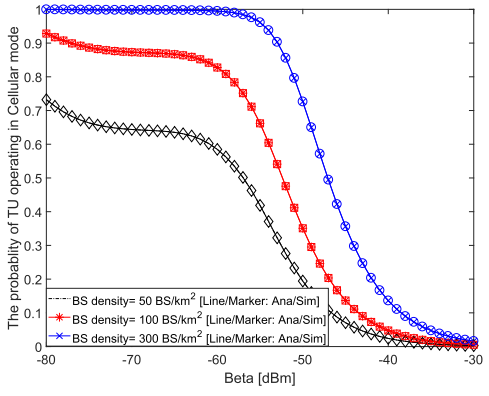

FIGURE 1. The probability for a TU to operate in the cellular mode vary the RSS threshold β, P_B = 24dBm.

Fig.1 illustrates the probability for a TU to operate in the cellular mode based on Eq.(17). It can be seen that the simulation results perfectly match the analytical results. From Fig.1, we can find that over 50% UEs can operate in the cellular mode when β is smaller than -57 dBm as the BS intensity is 50BS/km^2. This value increases by approximately to -52 dBm and -46 dBm when the BS intensity is 100BS/km^2 and 300BS/km^2, respectively. It indicates that the percentage of TU operating in cellular mode will increase as the BS intensity grows.

B. COVERAGE PROBABILITY

In this subsection, we investigate the coverage probability that a receiver's signal-to-interference-plus-noise ratio (SINR) is above a pre-designated threshold γ:

$$P_{Mode}\left(T, \lambda_{b,u}, \alpha_{B,D}\right) = \Pr\left[\text{SINR} > \gamma\right] \quad (18)$$

where γ is the SINR threshold, the subscript string variable *Mode* takes the value of 'Cellular' or 'D2D'. The SINR can be calculated as

$$\text{SINR} = \frac{P_D \zeta_{Mode}(r)\, y\left(\tilde{k}\right)}{I_{cellular} + I_{d2d} + N_0}, \quad (19)$$

where P_D and N_0 are the transmission power of each cellular and D2D UE transmitter and the additive white Gaussian noise (AWGN) power at each receiver, respectively. $I_{cellular}$ and I_{d2d} are the cumulative interference given by

$$I_{cellular} = \sum_{i:\, c_i \in \Phi_c \setminus signal} P_D \beta_i y\left(\tilde{k}\right)_i, \quad (20)$$

and

$$I_{d2d} = \sum_{j:\, d_i \in \Phi_{d2d} \setminus signal} P_D \beta_j y\left(\tilde{k}\right)_j, \quad (21)$$

where c_i and d_j are the i-th interfering CU and j-th interfering TU, β_i, β_j are the path loss associated with c_i and d_j, respectively. *signal* is the typical CU to BS link in the cellular mode and the typical TU to the RU link in the D2D mode. $y\left(\tilde{k}\right)$ is the channel gain on condition of the UE number $\tilde{k}$.

It is very important to note that the distribution of $y\left(\tilde{k}\right)$ should be derived according to (13). More specifically, we can reformulate (13) as

$$u^* = \underset{u \in \left\{1,2,\ldots,\tilde{k}\right\}}{\arg\max} \left\{\frac{\frac{P_D \zeta_B(r) h_u}{N_0}}{\frac{P_D \zeta_B(r) \times 1}{N_0}}\right\} = \underset{u \in \left\{1,2,\ldots,\tilde{k}\right\}}{\arg\max} \{h_u\}, \quad (22)$$

where h_u is an i.i.d. RV with a *unit-mean* exponential distribution due to our consideration of Rayleigh fading mentioned in Subsection III-A. Thus, $y\left(\tilde{k}\right)$ can be modeled as the maximum RV of $\tilde{k}$ i.i.d. exponential RVs. The complementary cumulative distribution function (CCDF) of $y\left(\tilde{k}\right)$ is [40]

$$\bar{F}_{Y\left(\tilde{k}\right)}(y) = Pr\left[Y\left(\tilde{k}\right) > y\right] = 1 - (1 - \exp(-y))^{\tilde{k}}. \quad (23)$$

It is easy to see that $Pr\left[Y\left(\tilde{k}\right) > y\right]$ increases as $\tilde{k}$ grows, which in turn improves the typical UE's channel gain. Note that for the round-robin (RR) scheduler, the typical UE is randomly selected in the BS. Consequently, we have that $\tilde{k} = 1$ in (23) and the analytical results for RR have been derived in [33].

1) COVERAGE PROBABILITY OF CELLULAR MODE

Based on the path loss model in Eq.(1) and the PF scheduler model in (13), we present our main result on $p_c^{\text{cov}}(\lambda,\gamma)$ in Theorem 2 and Theorem 3.

Theorem 2: Considering the path loss model in (1) and the PF scheduler model in (13), we can derive $p_c^{cov}(\lambda,\gamma)$ as

$$p_c^{cov}(\lambda,\gamma) = T_c^L + T_c^{NL}, \tag{24}$$

where

$$T_c^L = \int_{d_{n-1}}^{d_n} \mathbb{E}_{\left[\tilde{k}\right]}\left\{Pr\left[\frac{P_D\zeta_B^L(r)\,y\left(\tilde{k}\right)}{I_{cellular}+I_{d2d}+N_0}>\gamma\right]\right\} \times f_{R,n}^L(r)\,dr \tag{25}$$

and

$$T_c^{NL} = \int_{d_{n-1}}^{d_n} \mathbb{E}_{\left[\tilde{k}\right]}\left\{Pr\left[\frac{P_D\zeta_B^{NL}(r)\,y\left(\tilde{k}\right)}{I_{cellular}+I_{d2d}+N_0}>\gamma\right]\right\} \times f_{R,n}^{NL}(r)\,dr \tag{26}$$

where $n = \{1,2\}$, d_0 and d_2 are defined as 0 and $+\infty$, respectively. Moreover, $f_{R,n}^L(r)$ and $f_{R,n}^{NL}(r)$ $(d_{n-1} < r \le d_n)$, are represented by

$$f_{R,n}^L(r) = \exp\left(-\int_0^{r_1}\left(1-Pr_B{}^L(u)\right)2\pi u\lambda_b du - \int_0^{r} Pr_B{}^L(u)\,2\pi u\lambda_b du\right) Pr_B^L(r)\,2\pi r\lambda_b, \tag{27}$$

and

$$f_{R,n}^{NL}(r) = \exp\left(-\int_0^{r_2} Pr_B^L(u)\,2\pi u\lambda_b du - \int_0^{r}\left(1-Pr_B^L(u)\right)2\pi u\lambda_b du\right) \times\left(1-Pr_B^L(r)\right)2\pi r\lambda_b, \tag{28}$$

where $r_1 = \arg\limits_{r_1}\left\{\zeta_B^{NL}(r_1)=\zeta_B^L(r)\right\}$ and $r_2 = \arg\limits_{r_2}\left\{\zeta_B^L(r_2)=\zeta_B^{NL}(r)\right\}$.

Proof: See Appendix B. ■

Then, we will present the results of

$$\mathbb{E}_{\left[\tilde{k}\right]}\left\{Pr\left[\frac{P_D\zeta_B^L(r)\,y\left(\tilde{k}\right)}{I_{cellular}+I_{d2d}+N_0}>\gamma\right]\right\}$$

and

$$\mathbb{E}_{\left[\tilde{k}\right]}\left\{Pr\left[\frac{P_D\zeta_B^{NL}(r)\,y\left(\tilde{k}\right)}{I_{agg}+P_N}>\gamma\right]\right\}$$

in Theorem 3 as follows.

Theorem 3: Considering the truncated Negative Binomial distribution of the UE number per active BS, $\tilde{K}$, characterized in (10), we can derive $\mathbb{E}_{\left[\tilde{k}\right]}\left\{Pr\left[\frac{P_D\zeta_n^L(r)y\left(\tilde{k}\right)}{I_{agg}+P_N}>\gamma\right]\right\}$, which will be used in Theorem 2 as

$$\mathbb{E}_{\left[\tilde{k}\right]}\left\{Pr\left[\frac{P_D\zeta_B^L(r)\,y\left(\tilde{k}\right)}{I_{agg}+P_N}>\gamma\right]\right\} = \sum_{\tilde{k}=1}^{\tilde{K}^{max}}\left[1-\sum_{t=0}^{\tilde{k}}\binom{\tilde{k}}{t}\left(-\delta^L(r)\right)^t \mathscr{L}_{I_{cellular}}^L\left(\frac{t\gamma}{P_D\zeta_B^L(r)}\right) \times \mathscr{L}_{I_{d2d}}^L\left(\frac{t\gamma}{P_D\zeta_B^L(r)}\right)\right] f_{\tilde{K}}\left(\tilde{k}\right), \tag{29}$$

where $I_{agg} = I_{cellular} + I_{d2d}$, $\tilde{K}^{max}$ is a large enough integer that makes $F_{\tilde{K}}\left(\tilde{K}^{max}\right)$ in (11) close to one with a gap of a small value ϵ so that the expectation value in (19) can be accurately evaluated over $\tilde{k}$, $f_{\tilde{K}}\left(\tilde{k}\right)$ is obtained from (10), $\delta^L(r)$ is expressed by

$$\delta^L(r) = \exp\left(-\frac{\gamma N_0}{P_D\zeta_B^L(r)}\right), \tag{30}$$

and $\mathscr{L}_{I_{cellular}}^L(s)$ is the Laplace transform of $I_{cellular}$ for LoS signal transmission evaluated at s, which can be further written as

$$\mathscr{L}_{I_{cellular}}^L(s) = \exp\left(-2\pi\tilde{\lambda}\int_r^{d_B}\frac{Pr_B{}^L(u)\,u}{1+\left(sP_D\zeta_B^L(u)\right)^{-1}}du\right) \times \exp\left(-2\pi\tilde{\lambda}\int_{r_1}^{d_B}\frac{Pr_B{}^L(u)\,u}{1+\left(sP_D\zeta_B^L(u)\right)^{-1}}du\right) \times \exp\left(-2\pi\tilde{\lambda}\int_{d_B}^{+\infty}\frac{\left[1-Pr_B{}^L(u)\right]u}{1+\left(sP_D\zeta_B^{NL}(u)\right)^{-1}}du\right) \tag{31}$$

where $s = \frac{t\gamma}{P_D\zeta_B^L(r)}$ and $\mathscr{L}_{I_{d2d}}^L(s)$ is the Laplace transform of I_{d2d} for LoS signal transmission evaluated at s, which can be further written as

$$\mathscr{L}_{I_{d2d}}^L(s) = \exp\left(-2\pi\lambda_d\int_{\left(\frac{P_BA_{BL}}{\beta}\right)^{1/\alpha_{BL}}}^{d_B}\times\frac{Pr_B^L(u)\,u}{1+\left(sP_D\zeta_B^L(u)\right)^{-1}}du\right) \times \exp\left(-2\pi\lambda_d\int_{r_1}^{d_B}\frac{Pr_B^L(u)\,u}{1+\left(sP_D\zeta_B^L(u)\right)^{-1}}du\right) \times \exp\left(-2\pi\lambda_d\int_{d_B}^{+\infty}\frac{\left[1-Pr_B{}^L(u)\right]u}{1+\left(sP_D\zeta_B^{NL}(u)\right)^{-1}}du\right). \tag{32}$$

where $s = \frac{t\gamma}{P_D\zeta_B^L(r)}$

In a similar way, $\mathbb{E}_{\left[\tilde{k}\right]}\left\{Pr\left[\frac{P_D\zeta_B^{NL}(r)y\left(\tilde{k}\right)}{I_{agg}+P_N}>\gamma\right]\right\}$ *is computed by*

$$\mathbb{E}_{\left[\tilde{k}\right]}\left\{Pr\left[\frac{P_D\zeta_B^{NL}(r)\,y\left(\tilde{k}\right)}{I_{agg}+P_N}>\gamma\right]\right\}$$
$$=\sum_{\tilde{k}=1}^{\tilde{K}^{max}}\left[1-\sum_{t=0}^{\tilde{k}}\binom{\tilde{k}}{t}\left(-\delta^{NL}(r)\right)^t\times\mathscr{L}_{I_{agg}}^{NL}\left(\frac{t\gamma}{P_D\zeta_B^{NL}(r)}\right)\right]f_{\tilde{K}}\left(\tilde{k}\right),\tag{33}$$

where $\delta^{NL}(r)$ *is expressed by*

$$\delta_n^{NL}(r)=\exp\left(-\frac{\gamma N_0}{P\zeta_B^{NL}(r)}\right),\tag{34}$$

and $\mathscr{L}_{I_{cellular}}^{NL}(s)$ *is the Laplace transform of* $I_{I_{cellular}}$ *for NLoS signal transmission evaluated at s, which can be further written as*

$$\mathscr{L}_{I_{cellular}}^{NL}(s)$$
$$=\exp\left(-2\pi\tilde{\lambda}\int_{r_2}^{d_B}\frac{Pr_B{}^L(u)\,u}{1+\left(sP_D\zeta_B^L(u)\right)^{-1}}du\right)\times\exp\left(-2\pi\tilde{\lambda}\int_{r}^{d_B}\frac{\left[1-Pr_B{}^L(u)\right]u}{1+\left(sP_D\zeta_B^{NL}(u)\right)^{-1}}du\right)\times\exp\left(-2\pi\tilde{\lambda}\int_{d_B}^{+\infty}\frac{\left[1-Pr_B{}^L(u)\right]u}{1+\left(sP_D\zeta_B^{NL}(u)\right)^{-1}}du\right)\tag{35}$$

where $s=\frac{t\gamma}{P_D\zeta_B^{NL}(r)}$ *and* $\mathscr{L}_{I_{d2d}}^{NL}(s)$ *is the Laplace transform of* I_{d2d} *for NLoS signal transmission evaluated at s, which can be further written as*

$$\mathscr{L}_{I_{d2d}}^{L}(s)$$
$$=\exp\left(-2\pi\lambda_d\int_{r_2}^{d_B}\frac{Pr_B^L(u)\,u}{1+\left(sP_D\zeta_B^L(u)\right)^{-1}}du\right)\times\exp\left(-2\pi\lambda_d\int_{\left(\frac{P_BA_{BN}}{\beta}\right)^{1/\alpha_{BN}}}^{d_B}\times\frac{\left[1-Pr_B{}^L(u)\right]u}{1+\left(sP_D\zeta_B^{NL}(u)\right)^{-1}}du\right)\times\exp\left(-2\pi\lambda_d\int_{d_B}^{+\infty}\frac{\left[1-Pr_B{}^L(u)\right]u}{1+\left(sP_D\zeta_B^{NL}(u)\right)^{-1}}du\right)\tag{36}$$

where $s=\frac{t\gamma}{P_D\zeta_B^{NL}(r)}$.

Proof: See Appendix B. ■

From [17], T_c^L and T_c^{NL} are independent of each other. When the mode selection threshold β increases, we can find the intensity of D2D transmitter also increases. This will reduce the coverage probability performance of cellular tier, so we make $p_c^{cov}>\delta$ as a condition to guarantee the performance for the cellular mode when choosing β for the optimal system ASE. Although we have obtained the closed-form expressions of $p_c^{\text{cov}}(\lambda,\gamma)$ for the PF scheduler in Theorems 2 and 3, it is important to note that Theorem 3 is computationally intensive for the case of sparse networks, where the maximum UE number per active BS $\tilde{K}^{max}$ could be very large, leading to complex computations for $\mathscr{L}_{I_{agg}}^{L}\left(\frac{t\gamma}{P\zeta_B^L(r)}\right)$ and $\mathscr{L}_{I_{agg}}^{NL}\left(\frac{t\gamma}{P\zeta_B^{NL}(r)}\right), t\in\left\{0,1,\ldots,\tilde{K}^{max}\right\}$ in (29) and (33), respectively.

2) COVERAGE PROBABILITY OF THE TYPICAL UE IN THE D2D MODE

From [10], one can see that to derive the coverage probability of a generic D2D UE, we only need to derive the coverage probability for a typical D2D receiver UE. Similar to the analysis in subsection IV-B1, we focus on a typical D2D UE which is located at the origin o and scheduled to receive data from another D2D UE. Following Slivnyak's theorem for PPP, the coverage probability result derived for the typical D2D UE also holds for any generic D2D UE located at any location. In the following, we present the coverage probability for a typical D2D UE in Theorem 4.

Theorem 4: We focus on a typical D2D RU which is located at the origin o and scheduled to receive data from another D2D TU, the probability of coverage $p_{D2D}^{cov}(\lambda,\gamma)$ *can be derived as*

$$p_{D2D}^{cov}(\lambda,\gamma)=\begin{cases}T_D^L & when\ 0<l\le d_D\\ T_D^{NL} & l>d_D,\end{cases}\tag{37}$$

where

$$T_D^{L,NL}=\exp\left(-2\pi\tilde{\lambda}\int_0^{d_D}\frac{Pr_D^L(u)\,u}{1+\left(sP_D\zeta_D^L(u)\right)^{-1}}du\right)\times\exp\left(-2\pi\tilde{\lambda}\int_{d_D}^{+\infty}\frac{\left[1-Pr_D^L(u)\right]u}{1+\left(sP_D\zeta_D^{NL}(u)\right)^{-1}}du\right)\times\exp\left(-2\pi\lambda_d\int_0^{d_D}\frac{Pr_D{}^L(u)\,u}{1+\left(sP_D\zeta_D^L(u)\right)^{-1}}du\right)\times\exp\left(-2\pi\lambda_d\int_{d_D}^{+\infty}\frac{\left[1-Pr_D^L(u)\right]u}{1+\left(sP_D\zeta_D^{NL}(u)\right)^{-1}}du\right)\times\exp\left(-\frac{\gamma N_0}{P_D\zeta_D^L(l)}\right)\tag{38}$$

where $s=\frac{\gamma}{P_D\zeta_D^L(l)}$ *when* $0<l\le d_D$ *and* $s=\frac{\gamma}{P_D\zeta_D^{NL}(l)}$ *when* $l>d_D$.

Proof: See Appendix C. ■

V. SIMULATION AND DISCUSSION

In this section, we use numerical results to validate our results and analyze the performance of the D2D-enabled UL cellular network. To this end, we present the simulation parameters, the validation of Theorem 2 and 3 on the coverage probability, the performance impact of the mode selection threshold and the proportional fair scheduler on the coverage probability, the results of the area spectral efficiency in Section V-A, V-B, V-D, V-C, respectively.

A. SIMULATION SETUP

According to the 3GPP Long Term Evolution (LTE) specifications [41], we set the system bandwidth to 10MHz, carrier frequency f_c to 2GHz. The transmit power of each BS and each D2D transmitter are set to $P_B = 24$ dBm and $P_D = 24$ dBm, respectively. Moreover, the threshold for selecting cellular mode communication is $\beta = -80 \sim -30$dBm. The noise powers are set to -95 dBm (including a noise figure of 9 dB at the receivers). Besides, the CU density λ_u is set to 300 UEs/km^2, which leads to $q = 4.05$ in (7) and (8) [36]. The simulation parameters are summarized in Table 1.

TABLE 1. Simulation parameters.

Parameters	Values	Parameters	Values
BW	10MHz	f_c	2GHz
λ_u	300 UEs/km^2	N_0	-95 dBm
α_{BL}	2.09	A_{BL}	$10^{-4.11}$
α_{BN}	3.75	A_{BN}	$10^{-3.29}$
α_{DL}	2	A_{DL}	$10^{-3.845}$
α_{DN}	4	A_{DN}	$10^{-5.578}$
P_b	24 dBm	P_d	24 dBm

B. VALIDATION OF THEOREM 2 AND 3 ON THE COVERAGE PROBABILITY

1) VALIDATION OF ON THE COVERAGE PROBABILITY FOR CELLULAR TIER

In this subsection, we present Monte Carlo simulation results to investigate the coverage probability and validate the analytical results in Theorem 2.

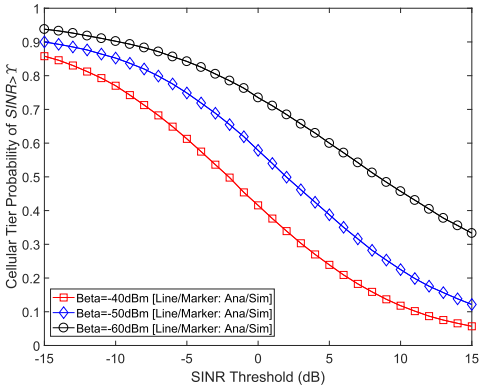

FIGURE 2. The Coverage Probability $p_c^{cov}(\lambda, \gamma)$ vs. SINR threshold ($\lambda_b = 100$ BSs/km^2, $\lambda_u = 300$ UEs/km^2, $\lambda_{TU} = 150$ UEs/km^2).

In Fig. 2, we plot the results of the coverage probability of cellular tier, we can draw the following observations:

- The analytical results of the coverage probability from Eq.(24) match well with the simulation results, which validates our analysis and shows that the adopted model accurately captures the features of the cellular tier in D2D-enhanced cellular networks.
- The coverage probability decreases with the increase of SINR threshold because a higher SINR requirement makes it more difficult to satisfy the coverage criterion in Eq.(18).
- For cellular tier, the coverage probability decreases as the interference management threshold beta increases because the larger beta, the more TU will operate in D2D mode and generate more interference to the cellular tier.

2) VALIDATION OF ON THE COVERAGE PROBABILITY FOR D2D TIER

In this subsection, we present Monte Carlo simulation results to investigate the coverage probability and validate the analytical results in Theorem 3, we set the distance l is 30m.

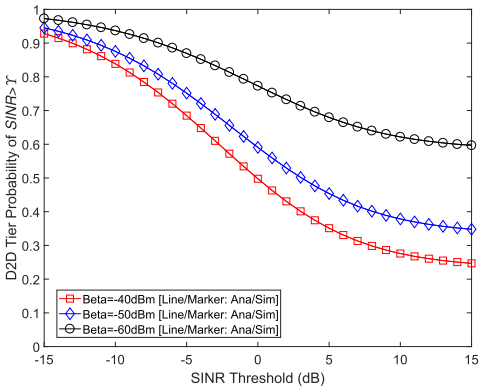

FIGURE 3. The Coverage Probability of D2D tier vs. SINR threshold ($\lambda_b = 100$ BSs/km^2, $\lambda_u = 300$ UEs/km^2, $\lambda_{TU} = 150$ UEs/km^2).

In Fig. 3, we plot the results of the coverage probability of the D2D tier, we can draw the following observations:

- The analytical results of the coverage probability from Eq.(37) match well with the simulation results, which validates our analysis and shows that the adopted model accurately captures the features of the D2D tier in D2D-enhanced cellular networks.
- For D2D tier, the coverage probability decreases as the interference management threshold beta increases because the larger beta, the more TU will operate in D2D mode and generate more interference to the D2D tier as well.

C. THE PERFORMANCE IMPACT OF PROPORTIONAL FAIR SCHEDULER ON THE COVERAGE PROBABILITY

In this subsection, we consider the proportional fair scheduler to investigate the performance impact of the proportional fair scheduler on the coverage probability.

To fully study the coverage probability with respect to the BS density with or without the PF scheduler, the results of coverage probability with various BS density and $\gamma_0 = 0$ dB are plotted in Fig 4. From this figure, we can draw the following observations:

- As predicted in Theorem 2, although the PF scheduler shows a better performance than the RR one for all BS

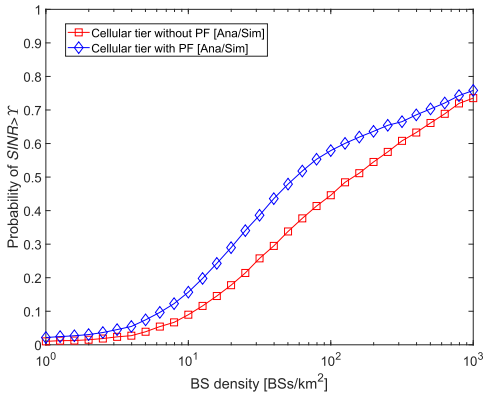

FIGURE 4. The Coverage Probability $p^{cov}(\lambda, \gamma)$ vs. BS density ($\gamma_0 = 0$ dB, $\lambda_u = 300$ UEs/km^2, $\lambda_{TU} = 150$ UEs/km^2, $\beta = 50$dBm).

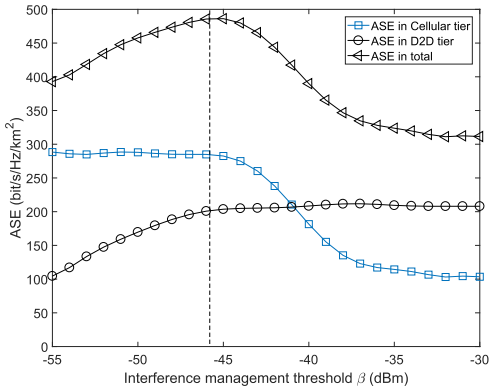

FIGURE 5. The ASE $A^{ASE}(\lambda, \gamma_0)$ vs. β ($\lambda_b = 100$ BSs/km^2, $\gamma_0 = 0$ dB, $\lambda_u = 300$ UEs/km^2, $\lambda_{Tu} = 150$ UEs/km^2).

densities, such performance gain diminishes as the network evolves into an UDN due to the loss of multi-user diversity. As can be seen from Fig. 4, the performance gain of the PF scheduler continuously decreases from around 100 % (ratio = 2) when $\lambda = 1$ BSs/km^2 toward zero (ratio = 1) in UDNs, e.g., $\lambda = 10^3$ BSs/km^2.

- The detailed explanation of the performance behavior in Fig. 4 is provided as follows:
  - When $\lambda \in [10^0, 10^1]$ BSs/km^2, the network is noise-limited, and thus the coverage probabilities of both RR and PF increase with the BS density λ as the network is lightened up with more BSs.
  - When $\lambda \in [10^1, 10^2]$ BSs/km^2, the increase rate of $p^{\text{cov}}(\lambda, \gamma)$ of the PF scheduler decrease. This is because *(i)* the signal power is enhanced by LoS transmissions, as shown by the $p^{\text{cov}}(\lambda, \gamma)$ of the RR scheduler in that BS density region; while *(ii)* the multi-user diversity decreases in that BS density region as exhibited in Fig. 4; and *(iii)* the above two factors roughly cancel each other out.
  - When $\lambda > 10^2$ BSs/km^2, the coverage probabilities of both RR and PF continuously increase. Such performance behavior can be attributed to the BS idle mode operations, i.e., *(i)* the signal power continues increasing with the network densification, and *(ii)* the interference power is controlled because not all BSs are turned on and emit interference.

D. THE PERFORMANCE IMPACT OF MODE SELECTION THRESHOLD ON THE ASE

In this subsection, we investigate the performance impact of mode selection threshold on the ASE and we find there exists an optimal beta that can achieve the maximum ASE of the D2D-enabled cellular network.

The analytical results of ASE with $\gamma_0 = 0$ dB vs various β values are shown in Eq.(15). Fig.5 illustrates the ASEs of Cellular links, D2D links and of the whole network with respect to different mode selection thresholds β. From this figure we can draw the following observations:

- When $\beta \in [-55dBm, -46dBm]$, the total ASE increases as the D2D links increases, because the D2D links do not generate a lot of interference to the cellular tier.
- An optimal β around -46 dBm which can achieve the maximum ASE there is a tradeoff between ASE increase for D2D links and ASE reduction for cellular links.
- When $\beta \in [-46dBm, -36dBm]$, the total ASE decreases because the D2D links generate more interference which makes the coverage probability of cellular UEs suffer. The ASE and the coverage probability of cellular links also decrease because the aggregate interference is now mostly LoS interference.
- When $\beta \in [-36dBm, -30dBm]$, the total ASE stay stable as well as the D2D ASE because the percentage of D2D UE is approaching 100%, which has been analyzed in Eq.(17).

From Fig.1, we can see that the additional D2D links make a significant contribution to the ASE performance and the D2D links will increase as β increase for all different densities of BS. At first, D2D links will enhance the ASE performance but they do not generate a lot of interference to the cellular tier. Then the increase of D2D transmitter will generate more interference which makes the coverage probability of cellular UEs suffer. The optimal β can be found in this stage for different densities of BS. At last stay stable as well as the D2D ASE because the percentage of D2D UE is approaching 100%. Above all, there exists an optimal β that can achieve the maximum ASE of the D2D-enabled cellular network while the coverage probability in the cellular tier is guaranteed. The mode selection threshold can control the interference from both cellular tier and D2D tier. In addition, the D2D tier can nearly double the ASE for the network when appropriately choosing the threshold for mode selection.

VI. CONCLUSION

In this paper, we proposed an interference management method in a D2D-enhanced uplink cellular network. In particular, each UE selects its operation mode based on its

downlink received power and a threshold β. With considering the PF scheduler, we studied the network performance of both the cellular tier and D2D tier. Using a stochastic geometric approach, analytical results that are computationally efficient have been derived for both the cellular tier and D2D tier. Our results showed that the interference management method mitigates large interference from D2D transmitter to the cellular network and the PF scheduler can improve the network performance significantly when the BS density is smaller than 10^{-3}BSs/km^2. Moreover, we concluded that D2D tier can improve the network performance when the threshold parameter is appropriately chosen and there exists an optimal β to achieve the maximum ASE while guaranteeing the coverage probability performance of the cellular network.

As our future work, we will consider other factors of realistic networks in the theoretical analysis for SCNs, such as practical directional antennas [2] and non-PPP deployments of BSs [42].

APPENDIX A
PROOF OF LEMMA 1

The probability that the RSS is larger than the threshold is given by

$$P = \Pr\left[\max_b \left\{P_b^{\text{rx}}\right\} > \beta\right], \tag{39}$$

where we use the standard power loss propagation model with a path loss exponent α_{BL} (for LoS UE-BS links) and α_{BN} (for NLoS UE-BS links).The probability that a generic mobile UE operates in the cellular mode:

$$\begin{aligned}
q &= 1 - \Pr\left[\max_b \left\{P_b^{\text{rx}}\right\} \le \beta\right] \\
&= 1 - \Pr\left[\max\left\{P_{LoS}^{rx}\right\} \le \beta \cap \max\left\{P_{NLoS}^{rx}\right\} \le \beta\right] \\
&= 1 - \Pr\left[\min R^{BL} \ge \left(\frac{P_B \mathrm{A}_{BL}}{\beta}\right)^{1/\alpha_{BL}}\right. \\
&\quad \left. \cap\ \min R^{BN} \ge \left(\frac{P_B \mathrm{A}_{BN}}{\beta}\right)^{1/\alpha_{BN}}\right] \\
&= 1 - \Pr\left[\text{no nodes within } \left(\frac{P_B \mathrm{A}_{BL}}{\beta}\right)^{1/\alpha_{BL}}\right. \\
&\quad \left. \cap\ \text{no nodes within } \left(\frac{P_B \mathrm{A}_{BN}}{\beta}\right)^{1/\alpha_{BN}}\right] \\
&= 1 - \exp\left[-\pi\lambda_b \int_0^{\left(\frac{P_B \mathrm{A}_{BL}}{\beta}\right)^{\frac{1}{\alpha_{BL}}}} {P_B}^L r dr\right] \\
&\quad \times \exp\left[-\pi\lambda_b \int_0^{\left(\frac{P_B \mathrm{A}_{BN}}{\beta}\right)^{\frac{1}{\alpha_{BN}}}} {P_B}^{NL} r dr\right],
\end{aligned} \tag{40}$$

which concludes our proof.

APPENDIX B
PROOF OF THEOREM AND THEOREM 3

By invoking the law of total probability, the coverage probability of cellular links can be divided into two parts, i.e., $T_c^L + T_c^{NL}$, which denotes the conditional coverage probability given that the typical CU is associated with a BS in LoS and NLoS, respectively. First, we derive the coverage probability for LoS link cellular tier. Conditioned on the strongest BS being at a distance r from the typical CU, probability of coverage is given by

$$\begin{aligned}
T_c^L &= \Pr\left[\text{SIN}R^L > \gamma \,|\text{LOS}\right] \\
&= \Pr\left[\frac{P_D \zeta_B^L(r)\, y\left(\tilde{k}\right)}{I_{cellular} + I_{d2d} + N_0} > \gamma \,|\text{LOS}\right] \\
&= \int_{d_{n-1}}^{d_n} \mathbb{E}_{\left[\tilde{k}\right]}\left\{Pr\left[\frac{P_D \zeta_B^L(r)\, y\left(\tilde{k}\right)}{I_{cellular} + I_{d2d} + N_0} > \gamma\right]\right\} \\
&\quad \times f_{R,n}^L(r)\, dr
\end{aligned} \tag{41}$$

where $n = \{1, 2\}$. d_0 and d_2 are defined as 0 and $+\infty$, respectively.

$$\begin{aligned}
&\mathbb{E}_{\left[\tilde{k}\right]}\left\{Pr\left[\frac{P_D \zeta_B^L(r)\, y\left(\tilde{k}\right)}{I_{cellular} + I_{d2d} + N_0} > \gamma\right]\right\} \\
&= \mathbb{E}_{\left[\tilde{k}\right]}\left\{Pr\left[y\left(\tilde{k}\right) > \gamma\left(\frac{I_{cellular} + I_{d2d} + N_0}{P_D \zeta_B^L(r)}\right)\right]\right\} \\
&= \mathbb{E}_{\left[\tilde{k}\right]}\left\{1 - \left[1 - \exp\left(-\gamma\left(\frac{I_{cellular} + I_{d2d} + N_0}{P_D \zeta_B^L(r)}\right)\right)\right]^{\tilde{k}}\right\} \\
&= \sum_{\tilde{k}=1}^{\tilde{K}^{max}} \left[1 - \sum_{t=0}^{\tilde{k}} \binom{\tilde{k}}{t} (-1)^t \right. \\
&\quad \left. \times \exp\left(-t\gamma\left(\frac{I_{cellular} + I_{d2d} + N_0}{P_D \zeta_B^L(r)}\right)\right)\right] f_{\tilde{K}}\left(\tilde{k}\right) \\
&= \sum_{\tilde{k}=1}^{\tilde{K}^{max}} \left[1 - \sum_{t=0}^{\tilde{k}} \binom{\tilde{k}}{t} (-1)^t \exp\left(-t\gamma\left(\frac{N_0}{P_D \zeta_B^L(r)}\right)\right)\right. \\
&\quad \left. \times \mathscr{L}_{I_{cellular}}^L\left(\frac{t\gamma}{P_D \zeta_B^L(r)}\right) \mathscr{L}_{I_{d2d}}^L\left(\frac{t\gamma}{P_D \zeta_B^L(r)}\right)\right] f_{\tilde{K}}\left(\tilde{k}\right) \\
&= \sum_{\tilde{k}=1}^{\tilde{K}^{max}} \left[1 - \sum_{t=0}^{\tilde{k}} \binom{\tilde{k}}{t} \left(-\delta^L(r)\right)^t \right. \\
&\quad \left. \times \mathscr{L}_{I_{cellular}}^L\left(\frac{t\gamma}{P_D \zeta_B^L(r)}\right) \mathscr{L}_{I_{d2d}}^L\left(\frac{t\gamma}{P_D \zeta_B^L(r)}\right)\right] f_{\tilde{K}}\left(\tilde{k}\right)
\end{aligned} \tag{42}$$

where $\delta^L(r)$ is expressed by

$$\delta^L(r) = \exp\left(-\frac{\gamma N_0}{P_D \zeta_B^L(r)}\right), \tag{43}$$

and $\mathscr{L}^L_{I_{cellular}}(s)$ is the Laplace transform of $I_{cellular}$ for LoS signal transmission evaluated at s, which can be further written as

$$\begin{aligned}
&\mathscr{L}^L_{I_{cellular}}(s) \\
&= \exp\left(-2\pi\tilde{\lambda}\int_r^{d_B} \frac{Pr_B{}^L(u)\,u}{1+\left(sP_D\zeta_B^L(u)\right)^{-1}}du\right) \\
&\quad\times \exp\left(-2\pi\tilde{\lambda}\int_{r_1}^{d_B} \frac{Pr_B{}^L(u)\,u}{1+\left(sP_D\zeta_B^L(u)\right)^{-1}}du\right) \\
&\quad\times \exp\left(-2\pi\tilde{\lambda}\int_{d_B}^{+\infty} \frac{\left[1-Pr_B{}^L(u)\right]u}{1+\left(sP_D\zeta_B^{NL}(u)\right)^{-1}}du\right)
\end{aligned} \tag{44}$$

and $\mathscr{L}^L_{I_{d2d}}(s)$ is the Laplace transform of I_{d2d} for LoS signal transmission evaluated at s, which can be further written as

$$\begin{aligned}
&\mathscr{L}^L_{I_{d2d}}(s) \\
&= \exp\left(-2\pi\lambda_d \times \int_{\left(\frac{P_B A_{BL}}{\beta}\right)^{1/\alpha_{BL}}}^{d_B} \frac{Pr_B^L(u)\,u}{1+\left(sP_D\zeta_B^L(u)\right)^{-1}}du\right) \\
&\quad\times \exp\left(-2\pi\lambda_d\int_{r_1}^{d_B} \frac{Pr_B^L(u)\,u}{1+\left(sP_D\zeta_B^L(u)\right)^{-1}}du\right) \\
&\quad\times \exp\left(-2\pi\lambda_d\int_{d_B}^{+\infty} \frac{\left[1-Pr_B{}^L(u)\right]u}{1+\left(sP_D\zeta_B^{NL}(u)\right)^{-1}}du\right).
\end{aligned} \tag{45}$$

The logic of the calculation of T_c^{NL} is similar to that of T_c^L. Which concludes our proof.

APPENDIX C
PROOF OF THEOREM 4

The typical D2D receiver has a distance of l to an active D2D transmitter. The coverage probability can be written as

$$\begin{aligned}
&T_D^L \\
&= \Pr\left[SINR^L > \gamma \,|\text{LOS}\right] \\
&= \Pr\left[\frac{P_D\zeta_D^L(l)\,h}{I_{cellular}+I_{d2d}+N_0} > \gamma \,|\text{LOS}\right] \\
&= \mathbb{E}_{[I_{agg}]}\left[\Pr\left[h > \frac{\gamma\left(I_{cellular}+I_{d2d}+N_0\right)}{P_D\zeta_D^L(l)}\,|\text{LOS}, I_{agg}\right]\right] \\
&= \mathbb{E}_{[I_{agg}]}\left\{\exp\left[-\frac{\gamma\left(I_{cellular}+I_{d2d}+N_0\right)}{P_D\zeta_D^L(l)}\right]\right\} \\
&= \exp\left(-2\pi\tilde{\lambda}\int_0^{d_D} \frac{Pr_D{}^L(u)\,u}{1+\left(sP_D\zeta_D^L(u)\right)^{-1}}du\right) \\
&\quad\times \exp\left(-2\pi\tilde{\lambda}\int_{d_D}^{+\infty} \frac{\left[1-Pr_D{}^L(u)\right]u}{1+\left(sP_D\zeta_D^{NL}(u)\right)^{-1}}du\right) \\
&\quad\times \exp\left(-2\pi\lambda_d\int_0^{d_D} \frac{Pr_D{}^L(u)\,u}{1+\left(sP_D\zeta_D^L(u)\right)^{-1}}du\right) \\
&\quad\times \exp\left(-2\pi\lambda_d\int_{d_D}^{+\infty} \frac{\left[1-Pr_D{}^L(u)\right]u}{1+\left(sP_D\zeta_D^{NL}(u)\right)^{-1}}du\right) \\
&\quad\times \exp\left(-\frac{\gamma N_0}{P_D\zeta_D^L(l)}\right)
\end{aligned} \tag{46}$$

where $s = \frac{\gamma}{P_D\zeta_D^L(l)}$. The logic of the calculation of T_D^{NL} is similar to that of T_D^L. Which concludes our proof.

REFERENCES

[1] Cisco Visual Networking Index. (2016). *Global Mobile Data Traffic Forecast Update, 2015–2020 White Paper*. [Online]. Available: http://goo.gl/ylTuVx
[2] D. López-Pérez, M. Ding, H. Claussen, and A. H. Jafari, "Towards 1 Gbps/UE in cellular systems: Understanding ultra-dense small cell deployments," *IEEE Commun. Surveys Tuts.*, vol. 17, no. 4, pp. 2078–2101, 4th Quart., 2015.
[3] A. Asadi, Q. Wang, and V. Mancuso, "A survey on device-to-device communication in cellular networks," *IEEE Commun. Surveys Tuts.*, vol. 16, no. 4, pp. 1801–1819, 4th Quart., 2014.
[4] *Further Enhancements to LTE Time Division Duplex (TDD) for Downlink-Uplink (DL-UL) Interference Management and Traffic Adaptation*, document TR 36.828, 3GPP, Jun. 2012.
[5] J. S. Roessler, "LTE-advanced (3GPP rel. 12) technology introduction white paper," Rohde & Shwarz, Munich, Germany, Feb. 2015.
[6] X. Lin, J. G. Andrews, and A. Ghosh, "Spectrum sharing for device-to-device communication in cellular networks," *IEEE Trans. Wireless Commun.*, vol. 13, no. 12, pp. 6727–6740, Dec. 2014.
[7] H. ElSawy, E. Hossain, and M.-S. Alouini, "Analytical modeling of mode selection and power control for underlay D2D communication in cellular networks," *IEEE Trans. Commun.*, vol. 62, no. 11, pp. 4147–4161, Nov. 2014.
[8] A. Ramezani-Kebrya, M. Dong, B. Liang, G. Boudreau, and S. H. Seyedmehdi, "Joint power optimization for device-to-device communication in cellular networks with interference control," *IEEE Trans. Wireless Commun.*, vol. 16, no. 8, pp. 5131–5146, Aug. 2017.
[9] N. Lee, X. Lin, J. G. Andrews, and R. W. Heath, Jr., "Power control for D2D underlaid cellular networks: Modeling, algorithms, and analysis," *IEEE J. Sel. Areas Commun.*, vol. 33, no. 1, pp. 1–13, Jan. 2015.
[10] J. Liu, H. Nishiyama, N. Kato, and J. Guo, "On the outage probability of device-to-device-communication-enabled multichannel cellular networks: An RSS-threshold-based perspective," *IEEE J. Sel. Areas Commun.*, vol. 34, no. 1, pp. 163–175, Jan. 2016.
[11] D. Marshall, S. Durrani, J. Guo, and N. Yang, "Performance comparison of device-to-device mode selection schemes," in *Proc. IEEE 26th Annu. Int. Symp. Pers., Indoor, Mobile Radio Commun. (PIMRC)*, Aug./Sep. 2015, pp. 1536–1541.
[12] A. Abdallah, M. M. Mansour, and A. Chehab, "A distance-based power control scheme for D2D communications using stochastic geometry," in *Proc. IEEE 86th Veh. Technol. Conf. (VTC-Fall)*, Sep. 2017, pp. 1–6.
[13] H. Min, J. Lee, S. Park, and D. Hong, "Capacity enhancement using an interference limited area for device-to-device uplink underlaying cellular networks," *IEEE Trans. Wireless Commun.*, vol. 10, no. 12, pp. 3995–4000, Dec. 2011.
[14] G. George, R. K. Mungara, and A. Lozano, "An analytical framework for device-to-device communication in cellular networks," *IEEE Trans. Wireless Commun.*, vol. 14, no. 11, pp. 6297–6310, Nov. 2015.
[15] S. Lv, C. Xing, Z. Zhang, and K. Long, "Guard zone based interference management for D2D-aided underlaying cellular networks," *IEEE Trans. Veh. Technol.*, vol. 66, no. 6, pp. 5466–5471, Jun. 2017.
[16] P. Mach, Z. Becvar, and T. Vanek, "In-band device-to-device communication in OFDMA cellular networks: A survey and challenges," *IEEE Commun. Surveys Tuts.*, vol. 17, no. 4, pp. 1885–1922, 4th Quart., 2015.
[17] M. Ding, P. Wang, D. López-Pérez, G. Mao, and Z. Lin, "Performance impact of LoS and NLoS transmissions in dense cellular networks," *IEEE Trans. Wireless Commun.*, vol. 15, no. 3, pp. 2365–2380, Mar. 2016.

[18] Y. J. Chun, S. L. Cotton, H. S. Dhillon, A. Ghrayeb, and M. O. Hasna, "A stochastic geometric analysis of device-to-device communications operating over generalized fading channels," *IEEE Trans. Wireless Commun.*, vol. 16, no. 7, pp. 4151–4165, Jul. 2017.

[19] M. Haenggi, *Stochastic Geometry for Wireless Networks*. Cambridge, U.K.: Cambridge Univ. Press, 2012.

[20] J. G. Andrews, F. Baccelli, and R. K. Ganti, "A tractable approach to coverage and rate in cellular networks," *IEEE Trans. Commun.*, vol. 59, no. 11, pp. 3122–3134, Nov. 2011.

[21] T. D. Novlan, H. S. Dhillon, and J. G. Andrews, "Analytical modeling of uplink cellular networks," *IEEE Trans. Wireless Commun.*, vol. 12, no. 6, pp. 2669–2679, Jun. 2013.

[22] H. Ding, X. Wang, D. B. da Costa, and J. Ge, "Interference modeling in clustered device-to-device networks with uniform transmitter selection," *IEEE Trans. Wireless Commun.*, vol. 16, no. 12, pp. 7906–7918, Dec. 2017.

[23] J. Liu, M. Sheng, L. Liu, Y. Shi, and J. Li, "Modeling and analysis of SCMA enhanced D2D and cellular hybrid network," *IEEE Trans. Commun.*, vol. 65, no. 1, pp. 173–185, Jan. 2017.

[24] S. Badri, M. Naslcheraghi, and M. Rasti, "Performance analysis of joint pairing and mode selection in D2D communications with fd radios," in *Proc. IEEE Wireless Commun. Netw. Conf. (WCNC)*, Apr. 2018, pp. 1–6.

[25] A. Omri and M. O. Hasna, "A distance-based mode selection scheme for D2D-enabled networks with mobility," *IEEE Trans. Wireless Commun.*, vol. 17, no. 7, pp. 4326–4340, Jul. 2018.

[26] M. Salehi, A. Mohammadi, and M. Haenggi, "Analysis of D2D underlaid cellular networks: SIR meta distribution and mean local delay," *IEEE Trans. Commun.*, vol. 65, no. 7, pp. 2904–2916, Jul. 2017.

[27] R. Margolies *et al.*, "Exploiting Mobility in Proportional Fair Cellular Scheduling: Measurements and Algorithms," *IEEE/ACM Trans. Netw.*, vol. 24, no. 1, pp. 355–367, Feb. 2016.

[28] Y. Cheng, P. Fu, Y. Ding, B. Li, and X. Yuan, "Proportional fairness in cognitive wireless powered communication networks," *IEEE Commun. Lett.*, vol. 21, no. 6, pp. 1397–1400, Jun. 2017.

[29] M.-R. Hojeij, C. A. Nour, J. Farah, and C. Douillard, "Waterfilling-based proportional fairness scheduler for downlink non-orthogonal multiple access," *IEEE Wireless Commun. Lett.*, vol. 6, no. 2, pp. 230–233, Apr. 2017.

[30] J.-G. Choi and S. Bahk, "Cell-throughput analysis of the proportional fair scheduler in the single-cell environment," *IEEE Trans. Veh. Technol.*, vol. 56, no. 2, pp. 766–778, Mar. 2007.

[31] J. Wu, N. B. Mehta, A. F. Molisch, and J. Zhang, "Unified spectral efficiency analysis of cellular systems with channel-aware schedulers," *IEEE Trans. Commun.*, vol. 59, no. 12, pp. 3463–3474, Dec. 2011.

[32] A. H. Jafari, D. López-Pérez, M. Ding, and J. Zhang, "Study on scheduling techniques for ultra dense small cell networks," in *Proc. IEEE VTC*, Sep. 2015, pp. 1–6.

[33] M. Ding, D. López-Pérez, G. Mao, P. Wang, and Z. Lin, "Will the area spectral efficiency monotonically grow as small cells go dense?" in *Proc. IEEE GLOBECOM*, Dec. 2015, pp. 1–7.

[34] M. Ding, D. López-Pérez, and G. Mao. (Apr. 2017). "A new capacity scaling law in ultra-dense networks." [Online]. Available: https://arxiv.org/abs/1704.00399v1

[35] S. Lee and K. Huang, "Coverage and economy of cellular networks with many base stations," *IEEE Commun. Lett.*, vol. 16, no. 7, pp. 1038–1040, Jul. 2012.

[36] M. Ding, D. López-Pérez, G. Mao, and Z. Lin, "Study on the idle mode capability with LoS and NLoS transmissions," in *Proc. IEEE Global Commun. Conf. (GLOBECOM)*, Dec. 2016, pp. 1–6.

[37] I. Gradshteyn and I. Ryzhik, *Table of Integrals, Series, and Products*, 7th ed. New York, NY, USA: Academic, 2007.

[38] F. Liu, J. Riihijärvi, and M. Petrova, "Robust data rate estimation with stochastic SINR modeling in multi-interference OFDMA networks," in *Proc. 12th Annu. IEEE Int. Conf. Sens., Commun., Netw. (SECON)*, Jun. 2015, pp. 211–219.

[39] E. Liu and K. K. Leung, "Expected throughput of the proportional fair scheduling over Rayleigh fading channels," *IEEE Commun. Lett.*, vol. 14, no. 6, pp. 515–517, Jun. 2010.

[40] M. Ding, D. López-Pérez, A. H. Jafari, G. Mao, and Z. Lin, "Ultra-dense networks: A new look at the proportional fair scheduler," in *Proc. IEEE Global Commun. Conf. (GLOBECOM)*, Dec. 2017, pp. 1–7.

[41] *Small Cell Enhancements for E-UTRA and E-UTRAN—Physical Layer Aspects*, document TR 36.872, 3GPP, Dec. 2013.

[42] M. Ding and D. López-Pérez, "On the performance of practical ultra-dense networks: The major and minor factors," in *Proc. 15th Int. Symp. Modeling Optim. Mobile, Ad Hoc, Wireless Netw. (WiOpt)*, May 2017, pp. 1–8.

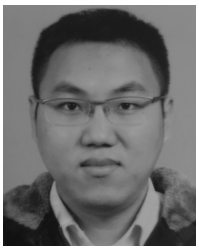

JUNNAN YANG (S'17) received the B.Eng. degree in electronics engineering and the M.Sc. degree in mechanical engineering from Zhejiang University, Zhejiang, China, in 2012 and 2015, respectively. He is currently pursuing the Ph.D. degree in engineering with the University of Technology Sydney. His research interests include 5G wireless communication networks, stochastic geometry, dense cellular networks, network performance analysis, intelligent transport systems, applied graph theory, and its applications in telecommunications.

MING DING (M'12–SM'17) received the B.S. and M.S. degrees (Hons.) in electronics engineering and the Ph.D. degree in signal and information processing from Shanghai Jiao Tong University (SJTU), Shanghai, China, in 2004, 2007, and 2011, respectively. From 2007 to 2014, he was with Sharp Laboratories of China, Shanghai, as a Researcher/Senior Researcher/Principal Researcher, where he also served as the Algorithm Design Director and the Programming Director for a system-level simulator of future telecommunication networks for more than seven years. He is currently a Senior Research Scientist with Data61, CSIRO, Sydney, NSW, Australia. He has authored over 80 papers in IEEE journals and conferences, all in recognized venues, and about 20 3GPP standardization contributions, as well as a Springer book *Multi-point Cooperative Communication Systems: Theory and Applications*. He holds 16 U.S. patents and co-invented over another 100 patents on 4G/5G technologies in Chinese, Japanese, and European. He was awarded, in 2017, as the Exemplary Reviewer of the IEEE TRANSACTIONS ON WIRELESS COMMUNICATIONS. He was the Lead Speaker of the industrial presentation on unmanned aerial vehicles in the IEEE Globecom 2017, which was awarded as the Most Attended Industry Program in the conference. He is currently an Editor of the IEEE TRANSACTIONS ON WIRELESS COMMUNICATIONS. Besides, he is or has been a Guest Editor/Co-Chair/Co-Tutor/TPC Member of several IEEE top-tier journals/conferences, e.g., the IEEE JOURNAL ON SELECTED AREAS IN COMMUNICATIONS, the *IEEE Communications Magazine*, and the IEEE Globecom Workshops.

GUOQIANG MAO (S'98–M'02–SM'08–F'18) was with the School of Electrical and Information Engineering, The University of Sydney. In 2014, he joined the University of Technology Sydney as a Professor of wireless networking and the Director of the Center for Real-Time Information Networks. He has published over 200 papers in international conferences and journals, which have been cited more than 7000 times. His research interests include intelligent transport systems, applied graph theory, and its applications in telecommunications, the Internet of Things, wireless sensor networks, wireless localization techniques, and network modeling and performance analysis. He is a Fellow of IET. He received the Top Editor Award for outstanding contributions to the IEEE TRANSACTIONS ON VEHICULAR TECHNOLOGY, in 2011, 2014, and 2015. He is a Co-Chair of the IEEE Intelligent Transport Systems Society Technical Committee on Communication Networks. He has served as the Chair, the Co-Chair, and a TPC Member of a number of international conferences. He has been an Editor of the IEEE TRANSACTIONS ON INTELLIGENT TRANSPORTATION SYSTEMS, since 2018, the IEEE TRANSACTIONS ON WIRELESS COMMUNICATIONS, since 2014, and the IEEE TRANSACTIONS ON VEHICULAR TECHNOLOGY, since 2010.

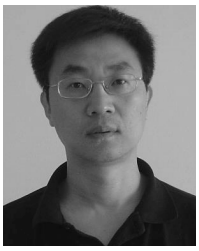

ZIHUAI LIN (S'98–M'06–SM'10) received the Ph.D. degree in electrical engineering from the Chalmers University of Technology, Sweden, in 2006. He held positions at Ericsson Research, Stockholm, Sweden. Following the Ph.D. graduation, he was a Research Associate Professor with Aalborg University, Denmark. He is currently with the School of Electrical and Information Engineering, The University of Sydney, Australia. His research interests include source/channel/network coding, coded modulation, MIMO, OFDMA, SC-FDMA, radio resource management, cooperative communications, small-cell networks, 5G cellular systems, and the IoT.

XIAOHU GE (M'09–SM'11) received the Ph.D. degree in communication and information engineering from the Huazhong University of Science and Technology (HUST), Wuhan, China, in 2003. Since 2005, he has been with HUST, where he is currently a Full Professor with the School of Electronic Information and Communications. He is an Adjunct Professor with the Faculty of Engineering and Information Technology, University of Technology Sydney, Ultimo, NSW, Australia. He is also the Director of the China International Joint Research Center of Green Communications and Networking.